

UNITED STATES  
DEPARTMENT OF THE INTERIOR  
GEOLOGICAL SURVEY

PREDICTED TIMING OF THE DISINTEGRATION OF THE LOWER REACH OF  
COLUMBIA GLACIER, ALASKA

by M. F. Meier<sup>1</sup>, L. A. Rasmussen<sup>1</sup>, Austin Post<sup>1</sup>, C. S. Brown<sup>1</sup>, W. G. Sikonja<sup>1</sup>,  
R. A. Bindschadler<sup>2</sup>, L. R. Mayo<sup>3</sup>, and D. C. Trabant<sup>3</sup>

---

Open-File Report 80-582

---

<sup>1</sup>USGS, Tacoma, WA

<sup>2</sup>NASA-Goddard Space Flight Center, Greenbelt, MD

<sup>3</sup>USGS, Fairbanks, AK

## CONTENTS

Executive Summary . . . . .	1
Symbols Used . . . . .	2
Introduction . . . . .	6
Calving Law . . . . .	7
General Observations on the Calving Glaciers of Alaska . . . . .	7
Data Relevant to the Calving Law . . . . .	10
Form of the Calving Law . . . . .	12
Flow Modeling . . . . .	14
Data Acquisition Program . . . . .	14
Data Adjustment Using the Continuity Equation . . . . .	16
Extension of the Data Net to the Calving Terminus . . . . .	19
The Dynamic Model . . . . .	21
The Calving Model . . . . .	25
A Perspective on the Prediction . . . . .	27
References . . . . .	30

## FIGURES

- Figure 1.--Index map of south-central and southeastern Alaska showing location of calving glaciers
- Figure 2.--Centerline water depth and calving speed for glaciers in table 2.
- Figure 3.--Map showing surface topography of lowest 16 km of Columbia Glacier.
- Figure 4.--Surface and bed profiles used in the calving model.
- Figure 5.--Cross-sectional area lost due to calving or to thinning.
- Figure 6. Longitudinal profile of the lowest 4 km of Columbia Glacier.
- Figure 7.--Longitudinal profile of velocity from the adjusted data set.
- Figure 8.--Predicted time profiles of terminus position and calving flux as functions of calving-law coefficient for 1978-88.

## TABLES

Table 1.--Current activity, width, and water depth at terminus; size; and accumulation-area ratio for 33 large calving glaciers of Alaska.

Table 2.--Water depth, ice surface height, calving speed, rate of advance, and buoyancy ratio at the termini of 12 glaciers.

Table 3.--Calving-law forms and coefficients, fitted to the data given in Table 2.

Predicted Timing of the Disintegration of the Lower  
Reach of Columbia Glacier, Alaska

by M. F. Meier<sup>1</sup>, L. A. Rasmussen<sup>1</sup>, Austin Post<sup>1</sup>, C. S. Brown<sup>1</sup>,  
W. G. Sikonja<sup>1</sup>, R. A. Bindschadler<sup>2</sup>, L. R. Mayo<sup>3</sup>,  
and D. C. Trabant<sup>3</sup>

EXECUTIVE SUMMARY

Grounded, iceberg-calving glaciers terminating in shallow water advance or retreat slowly; those terminating in deep (>80 m) water retreat rapidly (>.5 km/y, table 1). Columbia Glacier is retreating off a terminal-moraine shoal so that the water depth at its terminus is deepening with time. This report predicts that the rate of retreat of Columbia Glacier will accelerate during the next two or three years, and that the annual discharge of icebergs will increase to a peak of about 8-11 km<sup>3</sup>/y (6-8 times the 1978 value) in the period 1982 to 1985 (figure 8). This prediction has an uncertainty of timing of at least one year. The maximum rate of calving is expected to be in late summer. It is expected that the glacier will have retreated about 8 km by 1986, and that retreat will continue for several decades. This prediction could be refined markedly by comparing the predictions with new monitoring activities on the glacier.

---

<sup>1</sup>USGS, Tacoma, WA

<sup>2</sup>NASA-Goddard Space Flight Center, Greenbelt, MD

<sup>3</sup>USGS, Fairbanks, AK

This prediction is based on observations of all 52 calving glaciers in Alaska. Quantitative measurements of calving variables on 12 glaciers (table 2) yields a very simple calving law (figure 2, table 3): Calving speed (discharge/area) in  $m/y = 17 \pm 1$  times centerline water depth in m at terminus. This law was used in a new calving model based on mass continuity and an assumed, but glaciologically reasonable, future retracted profile. A dynamic model was used to confirm the calving model. The calving model results also match the present thinning and retreat of the glacier.

#### SYMBOLS USED

Symbol	Name	Dimensions
A	Parameter in ice flow law	$\text{bar}^{-n} \text{y}^{-1}$
a	Parameter in calving law	— or $m/y$
B	Vertical surface of a grid cell	$m^2$
b	Annual balance rate	$m/y$
c	Parameter in calving law	$y^{-1}$
$e_h$	Error in value of h or $h_w$	m
$e_v$	Error in value of $V_c$	$m/y$
F	Variance reduction fraction	
f	Velocity shape factor	
f*	Flux shape factor	
$G_0$	Glacier volume at time 0	$m^3$
$G_T$	Glacier volume at time T	$m^3$
g	Acceleration due to gravity	$m \text{ s}^{-2}$
h	Glacier thickness	m
$\dot{h}$	$dh/dt$	$m/y$

Symbol	Name	Dimensions
$h_f$	Thickness at floatation	m
$h_g$	Altitude at ice surface at terminus	m
$h_w$	Water depth at terminus	m
$\ell$	Boundary of grid cell on horizontal plane	m
$n$	Parameter in ice flow law	
$\mathbf{n}$	Outward-directed normal unit vector	
$0$	Initial time	y
$o$	Initial or unadjusted value	
$P$	Horizontal area of a grid cell	$m^2$
$Q$	Volume (total) flux	$m^3/y$
$Q_b$	Balance flux	$m^3/y$
$Q_c$	Calving flux	$m^3/y$
$Q_h$	Thickness-change flux	$m^3/y$
$\hat{Q}$	Volume flux per unit width at centerline	$m^2/y$
$Q^*$	Volume flux in stream sheet	$m^3/y$
$Q_e^*$	$Q$ at terminus	$m^3/y$
$\mathbf{Q}$	Volume flux vector	$m^3/y$
$R_b$	Residual in Equation 11a	$m^3/y$
$R_h$	Residual in Equation 11b	m
$R_x$	Residual in Equation 11c	$m/y$
$R_y$	Residual in Equation 11d	$m/y$
$S$	Cross-sectional area at terminus	$m^2$

Symbol	Name	Dimensions
$T$	Final time	$y$
$t$	Time	$y$
$V$	Speed at the surface	$m/y$
$V_b$	Basal sliding speed	$m/y$
$V_c$	Calving speed	$m/y$
$V_d$	Speed due to internal deformation	$m/y$
$V_x$	x-component of $\mathbf{V}$	$m/y$
$V_y$	y-component of $\mathbf{V}$	$m/y$
$\mathbf{V}$	Velocity vector at the surface	$m/y$
$W$	Width	$m$
$X$	Position of terminus on x-axis	$m$
$\dot{X}$	$dX/dt$	$m/y$
$x$	Horizontal coordinate in direction of flow	$m$
$y$	Horizontal coordinate perpendicular to $x$	$m$
$z$	Vertical coordinate directed up	$m$
$\alpha$	Surface slope angle	
$\gamma$	Ratio of $V$ to speed averaged through depth	
$\dot{\epsilon}$	Shear deformation rate	$y^{-1}$
$\zeta$	Horizontal coordinate orthogonal to $\xi$	$m$
$\xi$	Horizontal coordinate in direction of flow	$m$
$\xi$	Value of $\xi$ at terminus	$m$
$\rho_i$	Density of ice	$Mg/m^3$
$\rho_w$	Density of water	$Mg/m^3$

Symbol	Name	Dimensions
$\sigma_b$	Error in $P(\dot{b}-\dot{h})$	$m^3/y$
$\sigma_c$	Error in estimate of $c$	$y^{-1}$
$\sigma_h$	Error in $h$	$m$
$\sigma_x$	Error in $V_x$	$m/y$
$\sigma_y$	Error in $V_y$	$m/y$
$\tau$	Shear stress	bar
$\tau_b$	Local basal shear stress	bar
$\bar{\tau}_b$	Regional basal shear stress	bar
$\tau_{eff}$	Effective basal shear stress	bar
$\phi$	Variable used in Equation 5	varies
$\psi$	Variable used in Equation 5	varies
$\hat{\quad}$	(Superscript) designates value at centerline	

## INTRODUCTION

Nearly all grounded, iceberg-calving glaciers have experienced large-scale asynchronous advances and retreats. This behavior is apparently not directly related to climatic variations. The term calving glacier as used in this report refers to a glacier that ends in water and discharges icebergs but is grounded (not floating). A critical factor is the water depth at the terminus, as instability results when the glacier retreats even a short distance into a deep fiord or basin. The glacier may then retreat rapidly and irreversibly as unusual volumes of ice break away.

Columbia Glacier, near Valdez, Alaska, is a large calving glacier; it is 67 km long and 1,100 km<sup>2</sup> in area. It now ends on a moraine shoal in shallow water, but upglacier from the terminus the bed is about 400 m below sea level. Although the position of the terminus has been in a state of near equilibrium since 1794, evidence now suggests that rapid, drastic retreat may be imminent (Post, 1975; Meier and others, 1978; Meier and others, 1980). Small icebergs, bergy bits, and growlers drift from Columbia Glacier toward and occasionally into Valdez Arm. Drastic retreat would substantially increase the discharge of ice and would thus increase the iceberg hazard to shipping. In order to determine when this might happen and how much the iceberg discharge would be increased, an intensive study was begun by the Geological Survey in 1977.

This document presents a prediction of the iceberg-discharge rate to be expected in the next decade, together with brief descriptions of the analysis and modeling methods. For further information see Post, 1975; Meier and others 1978; Mayo and others, 1979; Sikonia and Post, 1979; Hodge, 1979; and Meier and others, 1980. Further documentation of the new methods and contributions to scientific knowledge resulting from this study will appear in forthcoming publications.

Prediction of the future discharge of icebergs from a calving glacier requires the solution of two interconnected problems. First, the future location of and the flow of ice to the terminus must be predicted. Second, the iceberg calving flux must be determined at the future terminus location. The first is a problem in glacier-flow dynamics, but an unusual one because the location and the geometry of the terminus depends on the rate of iceberg calving. A calving law, which relates the rate of calving at any instant to certain characteristics of the terminus at that instant, must be used as the terminus boundary condition for the ice flow analysis, and also must be used to provide estimates of the future iceberg discharge that are required for practical applications (Meier and others, 1978, p. 4, 5).

## CALVING LAW

### General Observations on the Calving Glaciers of Alaska

Of 52 tidewater iceberg-calving glaciers in Alaska, seven are currently advancing, 31 are stable, and 14 are retreating. Information on 33 large trunk glaciers is listed in table 1. These glaciers are scattered over southern and southeastern Alaska (figure 1). Between 1960

and 1980, aerial observations and photography, generally annual, were obtained of the terminus position and activity of all of these glaciers. During the field seasons of 1977, 1978, and 1979, the Geological Survey's Research Vessel Growler together with the radio-controlled skiff Bergy Bit were used to collect data on water depth at the termini of these same glaciers and in the bays and fiords formerly occupied by these glaciers (Post, 1980a, 1980b, 1980c, 1980d, 1980e, 1980f), and also served as a base for studies of recent glacial histories. These observational data show that:

(1) All glaciers with stable, advancing, or slowly retreating (<50 m/y) termini end in shallow water (generally less than 80 m) in either a retracted position (at the head of the bay or fiord) or in an advanced position ending on a terminal-moraine shoal. All glaciers that are presently at their retracted positions have retreated from advanced Neoglacial positions; the earliest of these drastic retreats occurred about 2,500 years ago, and the latest about 75 years ago. Only one glacier is still in an advanced position: Columbia.

(2) All glaciers that are or were rapidly retreating (0.5 to 10 km/y) end in water more than 80-m deep, and, in general, the deeper the water the faster the retreat. All of the glaciers observed in the process of rapid retreat had retreated from terminal-moraine shoals upon which they terminated not more than 100 years ago.

(3) The rate of retreat of a rapidly retreating glacier is also influenced by channel shape. Shallows, narrows, and sharp turns in the channel all reduce the rate of retreat; a temporary halt in the recession lasting several years may occur at such a location. As a result, a glacier

typically retreats by sudden, rapid recessions in broad, deep reaches interrupted by periods when the terminus is temporarily stationary where the channel is confined. As long as the water depth exceeds 80 m, however, calving ice is discharged more rapidly than it accumulates and the surface is lowered until the glacier makes another catastrophic recession to the next constriction in the channel.

(4) The advance of calving glaciers is relatively slow, generally about one to about three km per century. No calving glaciers have been observed advancing rapidly. The rate of advance is evidently controlled by how fast a terminal-moraine shoal can be moved ahead by erosion on the trailing slope and deposition on the leading slope. The internal structure of the moraine at Columbia Glacier is that of beds parallel to the leading slope, abruptly truncated at the trailing slope. This indicates that the moraine has been eroded on the trailing slope and sediment has been deposited on the leading slope.

(5) Advances or retreats of calving glaciers are not directly related to changing climate. This is indicated by: (a) Calving glacier variations are rarely synchronous with changes of other calving glaciers or with the variations of glaciers ending on land, whereas the latter generally occur simultaneously or at least in a consistent sequence. (b) The advances and retreats of calving glaciers show little relationship to their accumulation-area ratio (AAR), which is an index of mass balance. (c) The area and volume of calving glaciers change enormously between advanced and retracted positions, in some cases several-fold. (d) Various calving glaciers have made different numbers of advances and retreats during Neoglacial time, from only one to three or more.

Calving glaciers have advanced and retreated asynchronously for many centuries, the nature of the changes being controlled by the terminus properties and the configuration of the channel. Slow advances take place until the glacier reaches an extended position, where only a small retreat into deeper water behind the terminal shoal can trigger a drastic, irreversible retreat to the head of tidewater, whereupon a new cycle of slow advance commences.

#### Data Relevant to the Calving Law

The continuity equation for the terminus is written

$$S\dot{X} = Q - Q_C \quad (1)$$

where  $\dot{X}$  is the time rate of change of the position of the terminus  $X$  on the  $x$ -axis, which is horizontal and positive in the direction of the flow and has  $x=0$  at the head of the glacier;  $S$  is the area of the projection of the terminus onto a vertical plane normal to the  $x$ -axis;  $Q$  is the volume flux of ice to the terminus; and,  $Q_C$  is the iceberg calving flux from the terminus. The ratios  $Q/S \equiv V$  and  $Q_C/S \equiv V_C$  are defined to be, respectively, the average glacier speed at the terminus and the calving speed.

The calving law relates  $V_C$  to geometrical or other measurable properties of the terminus, so that  $Q_C$  can be calculated. The geometrical properties of the terminus thought to be most important include water depth  $h_w$  and ice-surface height  $h_g$ , where  $h = h_w + h_g$  is the total ice

thickness. Centerline (or maximum) values are here designated with (^); the absence of a superscript designates a total or an average over the width. Also of interest is how close the terminus is to floating, which can be measured by a buoyancy ratio  $\rho_w \hat{h}_w / \rho_i \hat{h}$  where  $\rho_w$  and  $\rho_i$  are the densities of water and ice, respectively.

Data sets were obtained for  $V$ ,  $\dot{X}$ ,  $h_g$ ,  $h_w$ , and  $S$  from recent observations on 12 important calving glaciers;  $Q$ ,  $Q_c$ , and  $V_c$  were then calculated. These results are listed in table 2.

Few of these data cover the upper range of values pertinent to a very rapid retreat phase of Columbia Glacier. Therefore a method was devised to estimate values of the variables from certain past rapid retreats, as follows. The continuity equation integrated over the entire glacier surface gives

$$\int_0^X (\dot{b} - \dot{h}) W dx = Q \quad (2)$$

where  $\dot{b}$  is the balance rate (in m of ice-equivalent per year) and  $\dot{h}$  is the time rate of change of the surface elevation (positive in the case of thickening), both measured in the vertical, and  $W$  is the width.

The integral in equation 2 can be partitioned into the sum of the balance flux  $Q_b$  and the thickness change flux  $Q_h$ ,

$$Q = Q_b + Q_h = \int_0^X \dot{b} W dx - \int_0^X \dot{h} W dx \quad (3)$$

The balance flux is calculated using a known  $\dot{b}(z)$  function. The only available  $\dot{b}(z)$  data for a maritime glacier in Alaska is that collected at Wolverine Glacier for 1966-1980. The average  $Q_b$  over the time interval

of measurement is taken to be the average of the integral evaluated at the beginning of the period of observation (time  $t = 0$ ) and that at the end of the period of observation ( $t = T$ ). Because  $\dot{b}(z)$  is not known at any other particular glacier, nor is its variation with time known,  $Q_b$  calculated this way is only a crude estimate. For the rapidly retreating glaciers of greatest interest here,  $Q_b$  is very small compared with  $Q_h$ , and only provides a small correction to the total flux.

The average thickness change flux  $Q_h$ , is determined from

$$Q_h = -(G_T - G_0)/(T - 0) \quad (4)$$

where  $G_0$  and  $G_T$  are the volumes of the glacier at  $t = 0$  and  $T$  respectively. The average calving flux is then calculated from equation 1, where  $S$  as well as  $h_g$  and  $h_w$  are taken to be averages over the distance of retreat from time 0 to time  $T$ . These results, listed in table 2 under method 2, are inherently less accurate than those taken from modern observations because of the averaging procedure.

#### Form of the Calving Law

An intuitive consideration of the stress distribution in the ice at the terminus of a calving glacier suggests that the calving speed is a function of some combination of the variables  $h_g$ ,  $h_w$ ,  $h$ , the force on the bed  $g(\rho_i h - \rho_w h_w)$  where  $g$  is the acceleration of gravity, and/or on the ice thickness necessary for flotation,  $h_f = \rho_w h_w / \rho_i$ . Thus the calving law is assumed to have the form

$$V_c = c\Phi/\Psi \quad (5)$$

where  $\Phi \equiv 1$ ,  $h$ ,  $h_w$ ,  $h_g$ , or  $h_f$ , and  $\Psi \equiv h$  or  $(\rho_i h - \rho_w h_w)$ , and  $c$  is a coefficient to be determined.

The possibility that calving is influenced by other variables such as accumulated strain, ice speed, water temperature, or state of the tide cannot be discounted. However, there is no direct evidence for Alaskan glaciers that these variables need to be separated explicitly. Studies at Columbia Glacier show that calving events are statistically uncorrelated with state of tide. On the other hand, seasonal runoff variations and lake-outburst events appear to cause sharply increased calving (Sikonia and Post, 1979). This difficulty is partly avoided here by considering only yearly averages; unpredictable future outbursts add some uncertainty to yearly average predictions.

Equation 5 was tested against the data shown in table 2. In addition, the function  $V_c = c(2\hat{h} - \hat{h}_w)$  and the two-parameter functions  $V_c = c(\hat{h} \text{ or } \hat{h}_w)^a$  and  $V_c = c\hat{h}_w + a$  were included in this study. The results are shown in table 3.

Surprisingly, one of the simplest of the possible calving laws

$$V_c = c\hat{h}_w \quad (6)$$

gives an excellent fit to the data, with a goodness of fit of 0.84. The best estimate of the coefficient  $c$  is  $17.0 \text{ y}^{-1}$ . The power-law regressions show that the best-fit relation is very close to linear, and the two-parameter linear relation shows that calving is approximately zero when the water depth is zero, further supporting the simple one-parameter,

one independent-variable calving law. This calving law and the data on which it is based are illustrated in figure 2.

Obviously, such a calving law cannot be correct for a floating glacier. None of the calving glaciers observed were floating; the ratio of floating thickness to actual thickness does not exceed 0.93 for those glaciers listed in table 2. The calving speed to be expected if one of these glaciers were to float is unknown. Greenland outlet glaciers with floating termini exhibit high calving speeds; in the case of Jacobshavn Glacier the calving speed exceeds 7 km per year.

## FLOW MODELING

### Data Acquisition Program

The speed of flow of a glacier depends, in general, on the thickness, surface slope, shape of channel, and the rheological properties of ice (e.g., Paterson, 1969). The discharge through a given cross section also is equal to the mass-balance rate minus the rate of change of thickness integrated over the surface area above that cross section (equation 2). The original objective of this project was to measure velocity, thickness, slope, bed topography, mass balance, and rate of change of thickness at a large number of points over the glacier in the hope that the numerical values of the flow-law parameters could be closely estimated and the modeling could be confidently carried out. Because of the complexity of this large glacier and some difficulties in the field work, it was not possible to achieve this level of determination of the flow modeling. Fortunately, sufficient data do exist so that gaps in coverage in important

areas can be filled in.

During the measurement year, defined as September 1, 1977, to August 30, 1978, a field program was undertaken to measure the flow, thickness, balance, and change in thickness at many points over Columbia Glacier (Meier and others, 1978; Mayo and others, 1979). Some measurement programs were extremely successful; for instance, surface velocity was measured about every 45 days at 200-300 points (Sikonia and Post, 1979). Some programs involved new procedures; for instance, mass-balance observations consider not only surface gains or losses and subsurface accumulation, but also subsurface melting due to loss of potential energy by the flowing ice (Mayo and others, 1979). Unfortunately, the ice-thickness measurement program, in spite of considerable effort, was not as successful; only about 110 good measurements could be obtained. Thus it was necessary to use velocity and other data to infer ice thickness over large areas.

The data requirements for this project are extremely stringent compared with those normally encountered in glacier modeling. Glacier models often begin with a prescribed bedrock configuration and a mass-balance function. The model then "grows" a simulated glacier; in the course of this growth over many simulated years, the condition of continuity and creep law of ice are obeyed. The resultant steady-state glacier is free of spurious transient effects. The Columbia Glacier prediction, on the other hand, begins with a markedly non-steady glacier, and then must simulate changes in the next ten years, as opposed to hundreds or thousands of years. If the data set does not obey continuity or the creep law throughout the solution region, then the ensuing simulation will include

spurious mass redistribution. Thus, a sophisticated and time-consuming data adjustment and balancing procedure was required.

### Data Adjustment Using the Continuity Equation

The volume flux  $Q$  through the cross section at  $x$  is given by

$$Q(x) = \int_0^W \int_0^h V(z) dz dy \cong \int_0^W \gamma h V dy \quad (7)$$

where  $V(z)$  is the magnitude at depth and  $V$  is the magnitude at the surface of the component of the velocity normal to the cross section, and  $\gamma$  is a parameter that relates  $V$  to the average value of the component over the vertical column. Combining this with equation 2 yields

$$\int_0^X (\dot{b} - \dot{h}) W dx \cong \int_0^W \gamma V h dy \quad (8)$$

The approximate value of  $\gamma$  can be inferred from other studies as about 0.85 except in those local areas where almost all of the flow is due to sliding. Equation 8 was used to adjust the inferred distribution of  $\dot{b}$  and  $\dot{h}$  in unmeasured areas above cross sections where  $h(y)$  is known.

Following this procedure, equation 8 was used to estimate thickness at cross sections where it could not be measured.

The data set resulting from this initial one-dimensional data adjustment was then used as input to a two-dimensional procedure. The continuity equation is written as

$$\dot{b} - \dot{h} = \nabla \cdot \mathbf{Q} \cong \gamma \nabla \cdot (\mathbf{V}h) \quad (9)$$

where  $\mathbf{Q}$  is the volume flux vector and  $\mathbf{V}$  the surface velocity vector. This was then calculated over each cell of a horizontal 71-by-63 grid of cell size = 762.5 m. Apparent flux divergence as high as 1000 m/y occurred when  $\mathbf{V}$  and  $h$  were taken from preliminary maps carefully prepared from the field data, yet  $\dot{b}-\dot{h}$  is generally less than 10 m/y. This indicates the need for incorporating two dimensions in the adjustment.

Considering a vertical column through a plan cell, the continuity equation in integral form is approximated as

$$\iint_{P_0} (\dot{b}-\dot{h})dP = \iint_{B_0} \mathbf{Q} \cdot \mathbf{n} dB \cong \oint_{\ell_0} \gamma h \mathbf{V} \cdot \mathbf{n} d\ell \quad (10)$$

where  $\mathbf{n}$  is the outward normal to the cell boundary,  $P$  is its area,  $B$  is the vertical column surface, and  $\ell$  is the boundary of the cell on a horizontal plane. The following observation equations are formed

$$\frac{1}{\sigma_b} \left[ \oint_{\ell_0} \gamma h \mathbf{V} \cdot \mathbf{n} d\ell - \iint_{P_0} (\dot{b}-\dot{h})dP \right] = \frac{R_b}{\sigma_b} \quad (11a)$$

for each cell, and

$$\frac{1}{\sigma_x} = [v_x - v_{x0}] = \frac{R_x}{\sigma_x} \quad (11b)$$

$$\frac{1}{\sigma_y} = [v_y - v_{y0}] = \frac{R_y}{\sigma_y} \quad (11c)$$

$$\frac{1}{\sigma_h} = [h - h_0] = \frac{R_h}{\sigma_h} \quad (11d)$$

for each grid point. Here  $\mathbf{V}=(v_x, v_y)$  and  $h$  are adjusted values of velocity and ice depth, and  $\mathbf{V}_0=(v_{x0}, v_{y0})$  and  $h_0$ , are the unadjusted values.

$\sigma_b$ ,  $\sigma_x$ ,  $\sigma_y$ , and  $\sigma_h$  are estimated errors associated with the continuity equation and with  $V_x$ ,  $V_y$ , and  $h$  that vary over the grid to account for spatial variation in observational quality and density.  $R_b$ ,  $R_x$ ,  $R_y$ , and  $R_h$  are the residuals and  $\dot{b}$  and  $\dot{h}$  are held fixed at the values resulting from the one-dimensional adjustment. Adjusted values  $V_x$ ,  $V_y$ , and  $h$  were then determined to minimize

$$\sum \left(\frac{R}{\sigma}\right)^2 \quad (12)$$

the sum running over all observation equations for all cells or grid points, and with  $R$  one of  $R_b$ ,  $R_x$ ,  $R_y$ , or  $R_h$ , and  $\sigma$  the corresponding one of  $\sigma$ ,  $\sigma_x$ ,  $\sigma_y$ , or  $\sigma_h$ . The  $\dot{b}$  and  $\dot{h}$  were adjusted slightly so that equation 10 was satisfied exactly when summed over the whole glacier, and the sum was equal to the total discharge from the terminus.

The result of this computation is a set of values of  $\dot{b}$ ,  $\dot{h}$ ,  $V_x$ ,  $V_y$ , and  $h$  that uses all measurement data and that is internally consistent with respect to the continuity equation, assuming  $\gamma$  to be constant. However, the flow law of ice is not necessarily obeyed. This slightly invalidates the agreement of the data through the continuity equation in that  $\gamma$  actually varies over the grid to accommodate the correct ice flow, including the presence of sliding at the bed.

## Extension of the Data Net to the Calving Terminus

Velocity and deformation increase rapidly as ice approaches to within 1000 m of the terminus of Columbia Glacier and could not be measured accurately, but ice surface altitude  $h_g$  and water depth  $h_w$  at the terminus were measured. Ice discharge along a transverse profile 2.81 km upglacier from the terminus is known for the 1977-78 measurement year to an accuracy of about 5 percent as a result of the two-dimensional adjustment. A horizontal curvilinear coordinate system for use in extending the flow data to the terminus was constructed so that the coordinate  $\xi$  everywhere follows the flow direction as defined by the adjusted data set;  $\zeta$  is the horizontal coordinate orthogonal to  $\xi$ .

The discharge component

$$\dot{Q}^* \equiv \Delta\zeta V h \gamma \quad (13)$$

is defined as the flow in a stream sheet bounded by two vertical surfaces parallel to the  $\xi$ -direction and separated by the width  $\Delta\zeta$ ; it is assumed that the velocity vectors at depth are parallel to those at the surface.  $\dot{Q}_0^*(\zeta)$  at  $\xi = 0$  is obtained by matching the two-dimensionally adjusted values at the transverse profile 2.81 km upglacier from the terminus. The terminus position  $\xi_e(\zeta)$  was measured from the six photogrammetric determinations during the measurement year and then averaged. Because  $\dot{Q}^*(\xi)$  is constant except for the gain or loss of material at the surface, the terminus discharge  $\dot{Q}_e^*(\zeta)$  is given by

$$\dot{Q}_e^*(\zeta) = \dot{Q}_0^*(\zeta) + \int_0^e \Delta\zeta (\dot{b} - \dot{h}) d\xi \quad (14)$$

Values of  $h_w$  and  $h_g$  were measured at  $\xi_e(\zeta)$ ; the average terminus advance  $\dot{\chi}(\zeta)$  was computed from

$$\dot{\chi}(\zeta) = \frac{1}{\Delta t} \left[ \xi_e(\zeta)_{8/26/78} - \xi_e(\zeta)_{8/29/77} \right] \quad (15)$$

At the terminus it is assumed that the speed at the surface equals that at depth, so ice speed  $V(\zeta)$  is obtained from

$$V(\zeta) = \dot{Q}_e^* / (h_w + h_g) \quad (16)$$

The calving speed  $V_c(\zeta)$  is defined by

$$V_c(\zeta) = V(\zeta) - \dot{\chi}(\zeta) \quad (17)$$

Values of  $Q$ ,  $\dot{\chi}$ ,  $V$ ,  $V_c$ ,  $h_w$ , and  $h_g$  at the terminus were then found integrating along the terminus face. Thus

$$Q = \int \dot{Q}_e^* d\zeta, \quad (18)$$

$$\dot{\chi} = \frac{1}{W} \int \dot{\chi} d\zeta,$$

and similarly for other variables. Also, average ice surface altitudes at  $\xi = 0, 1, 2,$  and  $2.5$  km were obtained from photogrammetric data at various times by similar integrations with respect to  $\zeta$ .

## THE DYNAMIC MODEL

Predictions of the future behavior of Columbia Glacier were made using a one-dimensional numerical model of temperate-glacier flow developed by Bindschadler (1978). This model has been used successfully in modeling the motion of the surge-type Variegated Glacier in Alaska and the calving Griesgletscher in Switzerland. For each time step, the model calculates the motion of the glacier at a series of transverse sections, and from mass continuity calculates how the surface will change.

Theory and experimental work indicate that the creep rate of ice can be expressed as

$$\dot{\epsilon} = A\tau^n \quad (19)$$

where  $\dot{\epsilon}$  is the shear deformation rate,  $\tau$  is the corresponding shear stress, and  $A$  and  $n$  are the flow-law parameters. Within the ice the shear stress at a vertical depth  $z$  is

$$\tau = \rho_i g z \sin \alpha \quad (20)$$

where  $\rho_i$  is the density of the ice,  $g$  is the acceleration due to gravity, and  $\alpha$  is the surface slope. When  $z=h$ , the ice thickness, equation 20 gives the maximum shear stress at the bed. This must be modified by a multiplicative shape factor,  $f$ , to give the average base stress over the complete transverse cross section (Nye, 1965),

$$\tau_b = f\rho_i g h \sin \alpha. \quad (21)$$

Longitudinal stresses within the ice can be partially accounted for by averaging the local base stress (equation 21) over a region larger than ten times the ice thickness. For a fine grid spacing, use of the regional base-stress results in a numerical instability of the model, making it necessary to compute an "effective base stress",

$$\tau_{\text{eff}} = .8 \bar{\tau} + .2 \tau_b \quad (22)$$

where  $\bar{\tau}_b$  is the regional base stress. This effective base stress linearly combines the regional and local stress values, preserving the basic smoothness of  $\bar{\tau}_b$  while allowing a numerically stable computation method.

Following customary practice (e.g., Paterson, 1969), equation 22 can be substituted into equation 19 and integrated from surface to bed giving

$$V = V_b + \frac{2Ah}{n+1} (f\rho gh \sin \alpha)^n = V_b + V_d \quad (23)$$

where  $V$  is the velocity at the surface,  $V_b$  is the sliding velocity at the bed, and  $V_d$  is the deformational velocity. Basal sliding, significant over the lower glacier, was calculated by forming the ratio  $\lambda = V_b/V$ . The proportionality of  $V_b$  to  $h\tau_{\text{eff}}^n$  corresponds closely to relationships suggested by Budd et al (1979) and Bindschadler (in preparation) where the effect of pressurized subglacial water is to cause increasing bed lubrication as the terminus is approached.

The volume flux is written as

$$Q = (f*V_d + \lambda V_b)S \quad (24)$$

where  $f^*V_d$  and  $\Lambda V_b$  are the deformation and sliding components of velocity, respectively, averaged over the entire cross-sectional area. The rate of ice-thickness change is obtained from the equation of continuity (equation 2):

$$\dot{h} = \dot{b} - \frac{1}{W} \frac{\Delta Q}{\Delta x} . \quad (25)$$

This parameterization of glacier dynamics has the advantage that  $f$  and  $f^*$  are insensitive to changes in glacier geometry and can therefore be considered constant in time. The sensitivities of  $\lambda$  and  $\Lambda$  are less well known but were also assumed constant in time.

The position of the terminus was determined from the calculated volume flux (equation 24), a calving speed calculated from equation 6, and the cross-sectional area. During test runs of the model it was found that an additional constraint had to be imposed to prevent a submerging terminus, a behavior which occurred during the catastrophic retreat phase. When the terminus thinned below the flotation thickness, the floating ice was removed from the glacier end. In addition, a fraction of this ice was added over the last glacier section to prevent any discontinuities in the calculated volume fluxes associated with the removal of the floating ice.

The dynamic analysis followed this order of calculation: Field measurements, adjusted by continuity according to equations 10-12, provided values of  $\dot{b}$  and  $\dot{h}$  so that equation 25 could be solved for  $\Delta Q/\Delta x$  and, assuming a boundary flux, integrated to calculate  $Q(x)$ . Values of the flow-law parameters,  $n=3$ ,  $A=.1 \text{ bar}^{-3} \text{y}^{-1}$  were assumed.

A profile of  $f(x)$  was estimated corresponding to theoretical values calculated for ice flow in a parabolic channel (Nye, 1965). Then by making the best possible initial estimates of  $h(x)$ ,  $V(x)$ ,  $f^*(x)$ ,  $\lambda(x)$ , and  $\Lambda(x)$  based on available data, these quantities were adjusted within specified error bounds to produce a set of profiles which satisfied equations 19 through 25. The non-linearity of the system (equation 19) resulted in a self-consistent solution without major alterations required within any of the profiles.

The region modeled was the lower 13.72 km of the glacier. Nineteen gridpoints were used at a spacing of 762.5 m. A constant volume flux of  $1.343 \text{ km}^3/\text{y}$  was specified at the head of this region. Values of the calving coefficient (equation 6) used were 14.739, 16.9, and  $20 \text{ y}^{-1}$ . The first value corresponds to an initial equilibrium of the terminus position while the latter two bound the region of  $c$  values deduced from measurements of other calving glaciers. Initially a time step of .01 y was used but during the catastrophic retreats this had to be reduced to .001 y (approximately 50 minutes) to allow the rapid retreat to be computed.

## THE CALVING MODEL

Another model was constructed in which the difficulty of properly applying the flow physics was not attempted. Instead, a glaciologically reasonable longitudinal profile for a retracted position is assumed; then, for any position of the terminus intermediate between its initial position and the retracted position, the corresponding longitudinal profile is simply interpolated between the initial longitudinal profile and the longitudinal profile assumed for the retracted position. Also assumed are two components of the flux at the upglacier end of the longitudinal profile for the retracted position: a flux that is constant in time and a reservoir drawdown volume that must be disposed of during the retreat by a flux that increases linearly in time. The model uses those two flux components along with equation 2 to determine the glacier flux to the terminus, equation 6 to determine the iceberg flux from the terminus, and equation 1 to determine the retreat rate.

This model was tested against McCarty Glacier 1942-50 data, a period when this glacier was undergoing rapid retreat. The resulting retreat scenario agrees with what is known about the glacier at that time.

The model was applied to the Columbia Glacier by assuming two different longitudinal profiles (from  $x = 52.6$  km to  $x = 57.1$  km; see figure 3) for the retracted position, one corresponding to a  $2.2 \text{ km}^3$  drawdown of ice above  $x = 52.6$  km and the other to  $10.0 \text{ km}^3$  (figures 4, 5).

Columbia Glacier is presently thinning, and the rate of thinning is increasing with time (figure 6) (Sikonia and Post, 1979; Meier and others, 1980). Also, thinning increases downglacier except within one kilometer of the terminus. The increase in thinning causes an increase in slope, which produced a slight but measurable increase in velocity from 1977 to 1978; from 1978 to 1979 the velocity remained about constant or decreased slightly (figure 7). From 1976 to 1979 the terminus position retreated about 180 m.

The predicted time profiles of terminus position  $X$  and calving flux  $Q_c$  are shown in figure 8 for the  $10.0 \text{ km}^3$  drawdown, for  $c = 15, 17, 19,$  and  $21 \text{ y}^{-1}$ . The effect of numerical error was nearly eliminated by examining the computations for grid spacings of  $\Delta x = 500 \text{ m}, 250 \text{ m},$  and  $100 \text{ m}$ .

The variation in the predicted profiles of terminus position and calving flux is obtained by varying  $c$  over a range of values that is broader than the likely range indicated in the estimation of that coefficient from studying all the other glaciers. However, other uncertainties in the calculations, such as errors in the bed topography or changes in the mass balance, should be accommodated by taking the entire range exhibited in figure 8 as representing the probable error in the predictions of  $X(t)$  and  $Q_c(t)$ . When the computed terminus retreat rates for the  $2.2 \text{ km}^3$  drawdown case and the  $10.0 \text{ km}^3$  drawdown case are compared with the observed retreat of the terminus since 1978, it is apparent that only the  $10.0 \text{ km}^3$  case gives reasonable rates.

## A PERSPECTIVE ON THE PREDICTION

Dynamic modeling suggests that the retreat rate and thus the calving flux may not increase as fast during the initial phase as is indicated by the calving model. During this period the glacier thins at the terminus and steepens; the increased slope causes a velocity increase which is almost sufficient to balance the speed of calving, but such a condition cannot continue indefinitely. Drastic retreat and high calving fluxes would be expected to occur before, or in the extreme case when, the ice thickness decreases to the point of floating. The predicted times, retreat rates, and calving fluxes for this extreme case are illustrated in figure 8. Alternatively, one might expect drastic retreat to occur when the ice cliff height is reduced to or below the 80-90 m height commonly observed at large calving glaciers. This produces a retreat rate faster than predicted by the calving model and faster than has been observed. The curve based on the initiation of floating can be considered as an indication of the maximum time before catastrophic retreat ensues. It is interesting that this occurs, for  $c \approx 17 \text{ y}^{-1}$ , at the same time as the maximum of calving flux (or greatest rate of retreat) predicted by the calving model. The initial retreat rates calculated by the dynamic model and by assuming the constant ice-cliff height criteria bracket the prediction given by the calving model, lending additional credence to the calving model.

The calving model predicts that the iceberg discharge from Columbia Glacier will increase to a peak in the period 1982-85, and that the peak discharge will be in the range of 8-11 km<sup>3</sup>/y, about 6-8 times the 1978

discharge. By 1986 the glacier will have retreated about 8 km, and the iceberg discharge will have decreased to about three times that of 1978. Retreat will then continue for several decades.

Unfortunately, it is not possible to define the timing of the drastic retreat more precisely. This is due in part to inaccuracies in the basic data and the simplifications and approximations to complex physical processes involved in the models. The ablation rate on the ice tongue in the next few years may be very different from that measured in 1977-78 (the 1979-80 winter was the snowiest on record), which will affect the timing of retreat. Perhaps most important, ice flow, calving, mass balance, and many other variables have very pronounced seasonal fluctuations. For instance, the calving flux averaged over periods of about 45 days in 1976-78 fluctuated between 0.5 and 2.8 km<sup>3</sup>/y. Yearly-averaged data were used in the models, causing an inherent error in timing of about 0.5 y. Due to the seasonality of calving, rapid retreat is likely to occur in late summer, but predicting the exact year is more difficult.

The calving flux predictions given in figure 8 are smooth curves. It must be understood that not only should a seasonal fluctuation be superimposed on them, but also that calving is very sporadic and episodic. Thus days will go by with very little calving; in other days the calving may be orders of magnitude more intense. These fluctuations will raise the peak calving fluxes far beyond those shown in figure 8.

As the glacier retreats, the terminal-moraine bar will form a natural barrier which will prevent the escape of extremely large icebergs. Bathymetric surveys of the moraine bar found water depths varying from awash to a maximum of 23 m at lower low water (Post, 1975), thus limiting the size of escaping bergs to those having a draft of less than 30 m. Larger bergs presently strand on the moraine, generally breaking into smaller fragments within a few hours which then drift over the moraine. The largest bergs noted outside of the barrier have been about 100 m in their longest dimension, corresponding to a weight of about 100,000 tons. Even bergs of this size melt rapidly in Prince William Sound; no bergs have been observed to survive more than a week, and no bergs have been observed at distances greater than about 30 km from the glacier. Although limiting the size and the distance icebergs can drift, the presence of the moraine will not greatly restrict the discharge of icebergs. Thus rather than few giant bergs drifting out of Columbia Bay as they are released from the glacier, much larger numbers of smaller icebergs will be released over the moraine shoal more frequently.

The model results include prediction of slow retreat during the initial few years. A careful monitoring program, begun soon, could check these initial predictions. This would allow the predictions of rapid retreat and calving flux to be considerably refined.

## REFERENCES

- Bindschadler, Robert Alan, 1978, A time-dependent model of temperate glacier flow and its application to predict changes in the surge-type Variegated Glacier during its quiescent phase: Unpublished thesis, University of Washington Geophysics Program, Seattle Washington, 244 p.
- Budd, W. F., Keage, P. L., and Blundy, N. A., 1979, Empirical studies of ice sliding: *Journal of Glaciology*, v. 23, no. 89, p. 157-170.
- Hodge, Steven M., 1979, Instability of a calving glacier terminus: *Journal of Glaciology*, v. 4, no. 90, p. 504.
- Mayo, L. R., Trabant, D. C., March, Rod, and Haerberli, Wilfried, 1979, Columbia Glacier stake location, mass balance, glacier surface altitude, and ice radar data, 1978 measurement year: U. S. Geological Survey Open-File Report 79-1168, 72 p.
- Meier, M. F., Post, Austin, Brown, C. S., Frank, David, Hodge, S. M., Mayo, L. R., Rasmussen, L. A., Senear, E. A., Sikonia, W. G., Trabant, D. C., and Watts, R. D., 1978, Columbia Glacier progress report--December 1977: U. S. Geological Survey Open-File Report 78-264, 56 p.
- Meier, M. F., Post, A., Rasmussen, L. A., Sikonia, W. G., and Mayo, L. R., 1980, Retreat of Columbia Glacier--a preliminary prediction: U. S. Geological Survey Open-File Report 80-10, 9 p.
- Nye, J. F., 1965, The flow of a glacier in a channel of rectangular, elliptic or parabolic cross-section: *Journal of Glaciology*, v. 5, no. 41, p. 661-690.
- Paterson, W. S. B., 1969, *The physics of glaciers*: New York, Pergamon Press, 250 p.
- Post, Austin, 1975, Preliminary hydrography and historic terminal changes of Columbia Glacier, Alaska: U. S. Geological Survey Hydrologic Investigations Atlas 559, 3 sheets.
- Post, Austin, 1980a, Preliminary bathymetry of Northwestern Fiord and neoglacial changes of Northwestern Glacier, Alaska: U. S. Geological Survey Open-File Report 80-414, 2 sheets.
- \_\_\_\_\_, 1980b, Preliminary bathymetry of Blackstone Bay and neoglacial changes of Blackstone Glacier, Alaska: U. S. Geological Survey Open-File Report 80-418, 2 sheets.

## REFERENCES

- \_\_\_\_ 1980c, Preliminary bathymetry of Aialik Bay and neoglacial changes of Aialik and Pederson Glaciers, Alaska: U. S. Geological Survey Open-File Report 80-423, 1 sheet.
- \_\_\_\_ 1980d, Preliminary bathymetry of McCarty Fiord and neoglacial changes of McCarty Glacier, Alaska: U. S. Geological Survey Open-File Report 80-424, 4 sheets.
- \_\_\_\_ 1980e, Preliminary bathymetry--Esther Passage to Eaglek Island, Alaska: U. S. Geological Survey Open-File Report 80-426, 1 sheet.
- \_\_\_\_ 1980f, Preliminary bathymetry--approaches to Unakwik Inlet, Alaska: U. S. Geological Survey Open-File Report 80-428, 1 sheet.
- Sikonia, William G., and Post, Austin, 1979, Columbia Glacier, Alaska: recent ice loss and its relationship to seasonal terminal embayments, thinning, and glacier flow: U. S. Geological Survey Open-File Report 79-1265, 2 sheets.

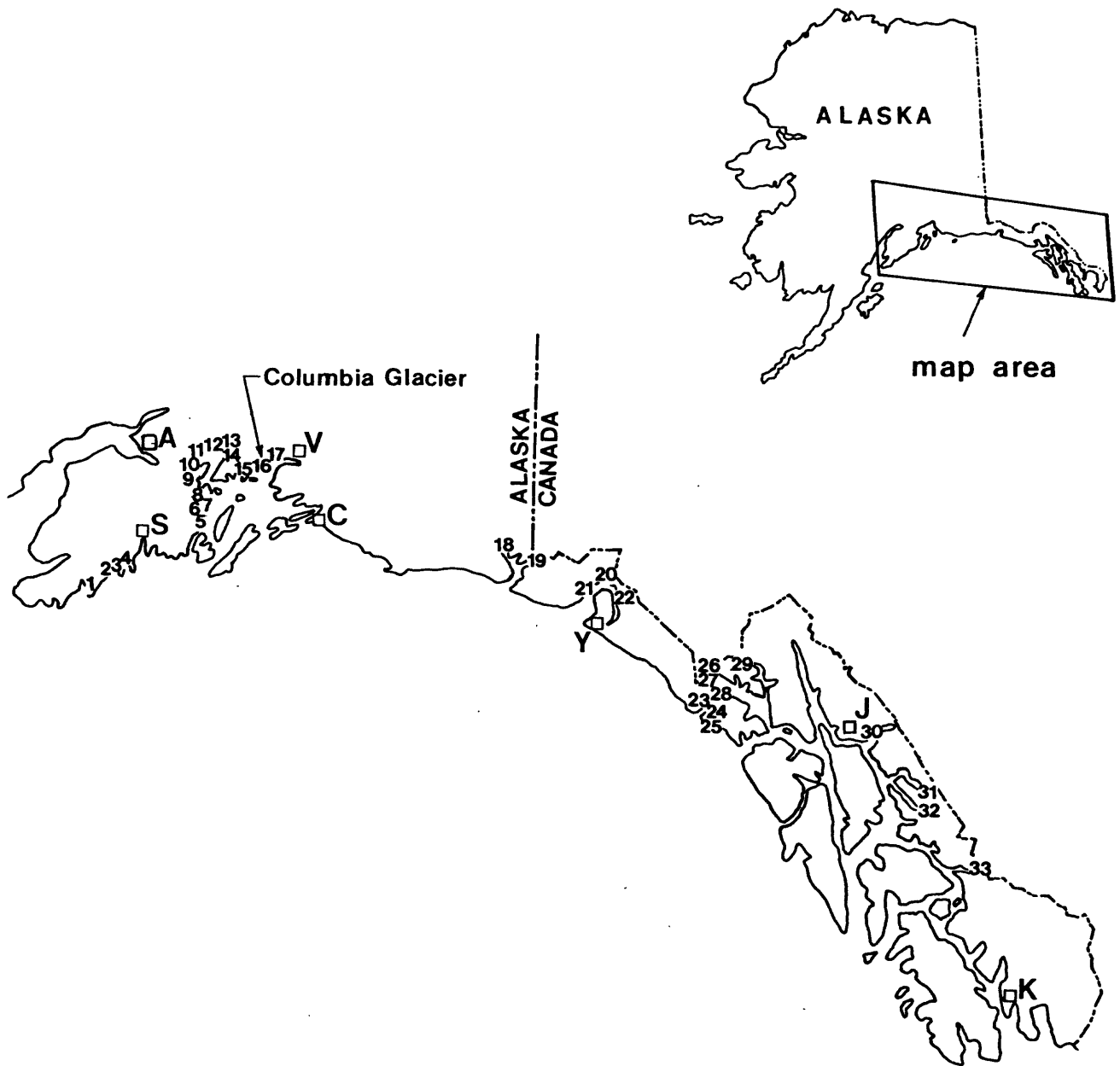


Figure 1.--Index map of south-central and southeastern Alaska showing location of calving glaciers. The numbers refer to tables 1 and 2. Cities and towns are indicated by A (Anchorage), C (Cordova), J (Juneau), K (Ketchikan), S (Seward), Y (Yakutat), and V (Valdez).

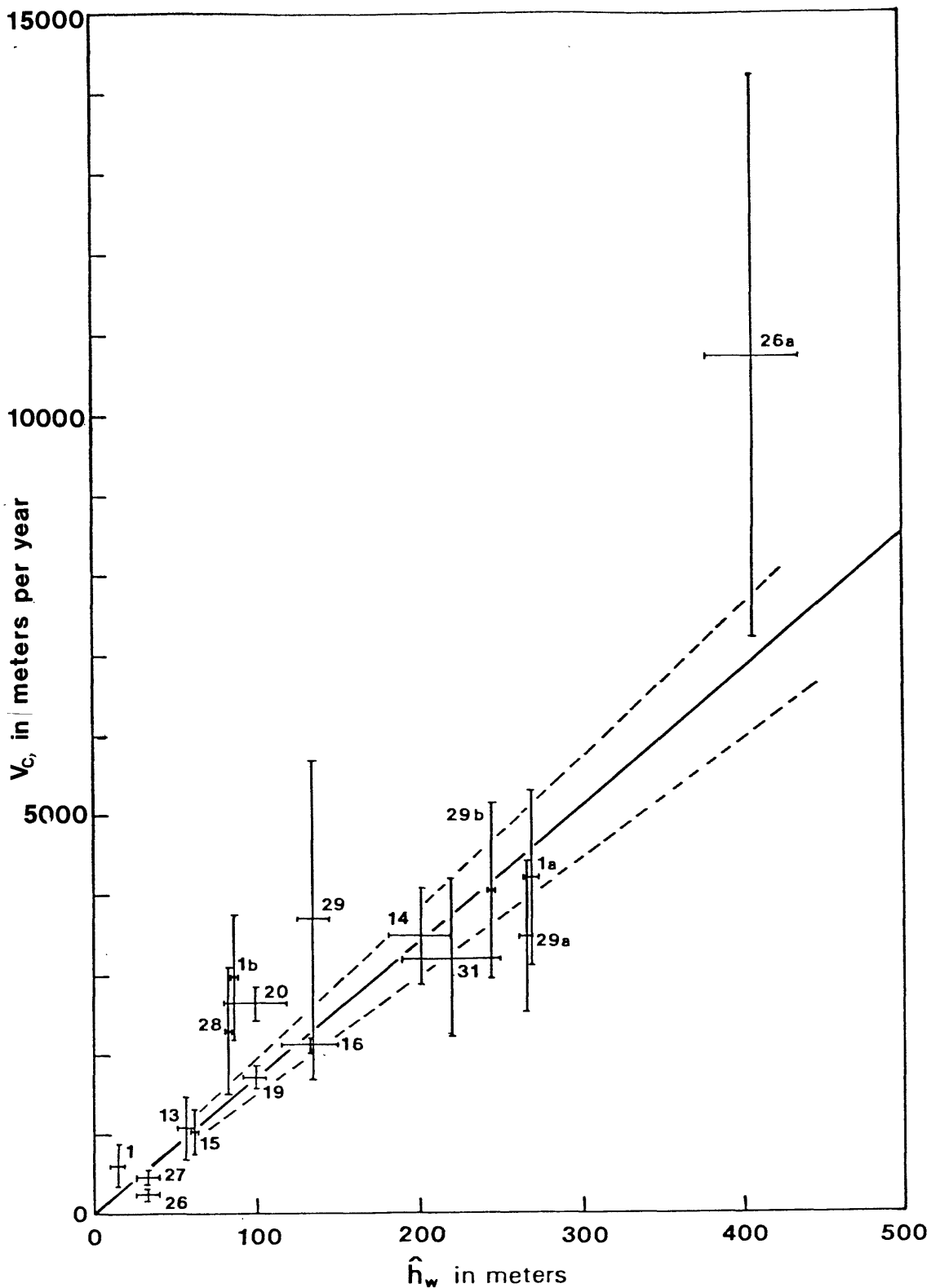


Figure 2.--Centerline water depth  $\hat{h}_w$  and calving speed  $V_c$  for the glaciers listed in table 2, together with the regression line (solid) corresponding to  $c=17.0$ , with 95 percent confidence limits (dashed). Error bars correspond to  $\pm$ one standard deviation.

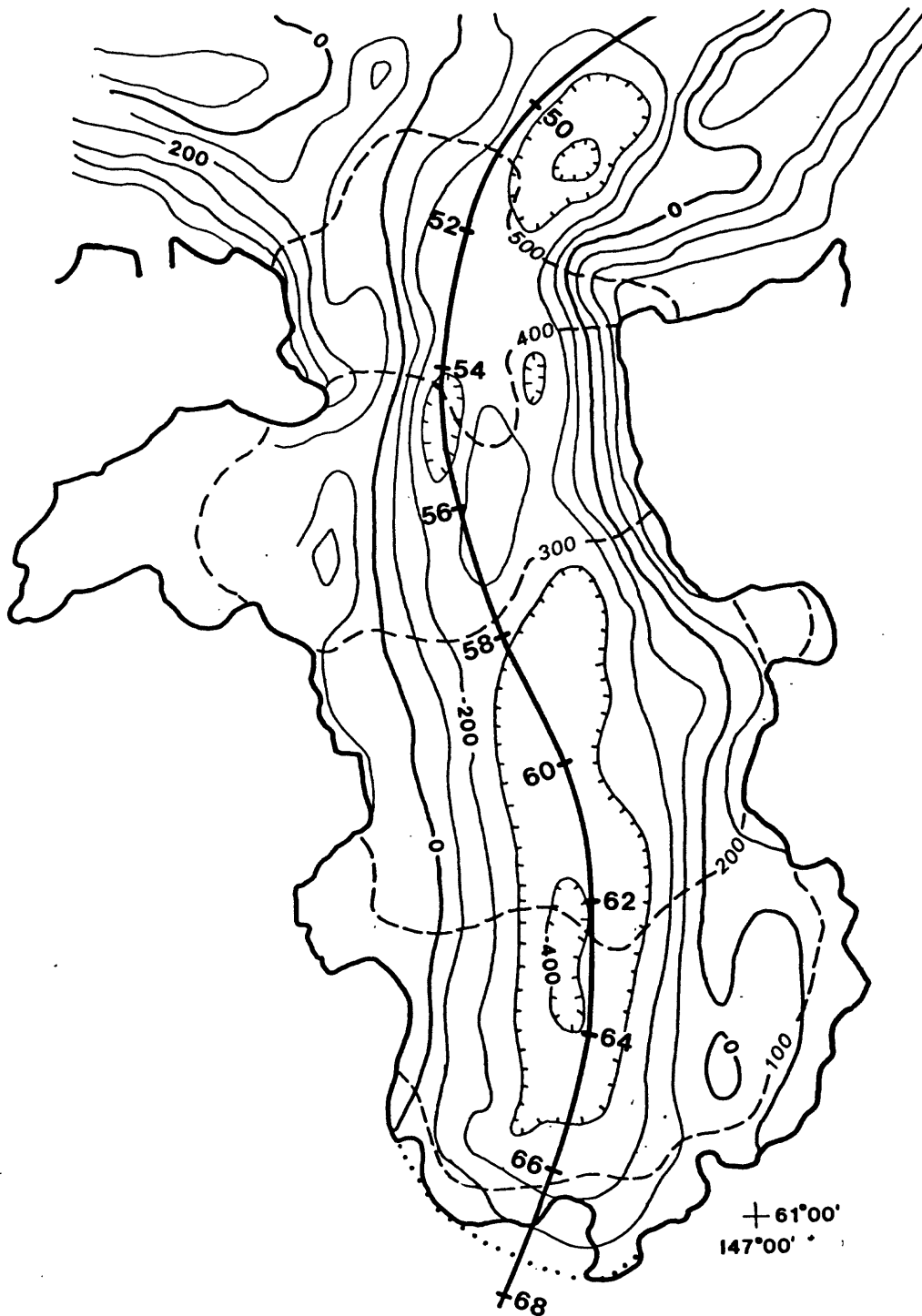


Figure 3.--Map showing surface (dashed lines) and bed (solid lines) topography for the lowest 16 kilometers of Columbia Glacier. Also shown is the longitudinal coordinate system (heavy line) and the position of the crest of the moraine shoal (dotted line). The terminus is shown as of the end of the 1977-78 measurement year.

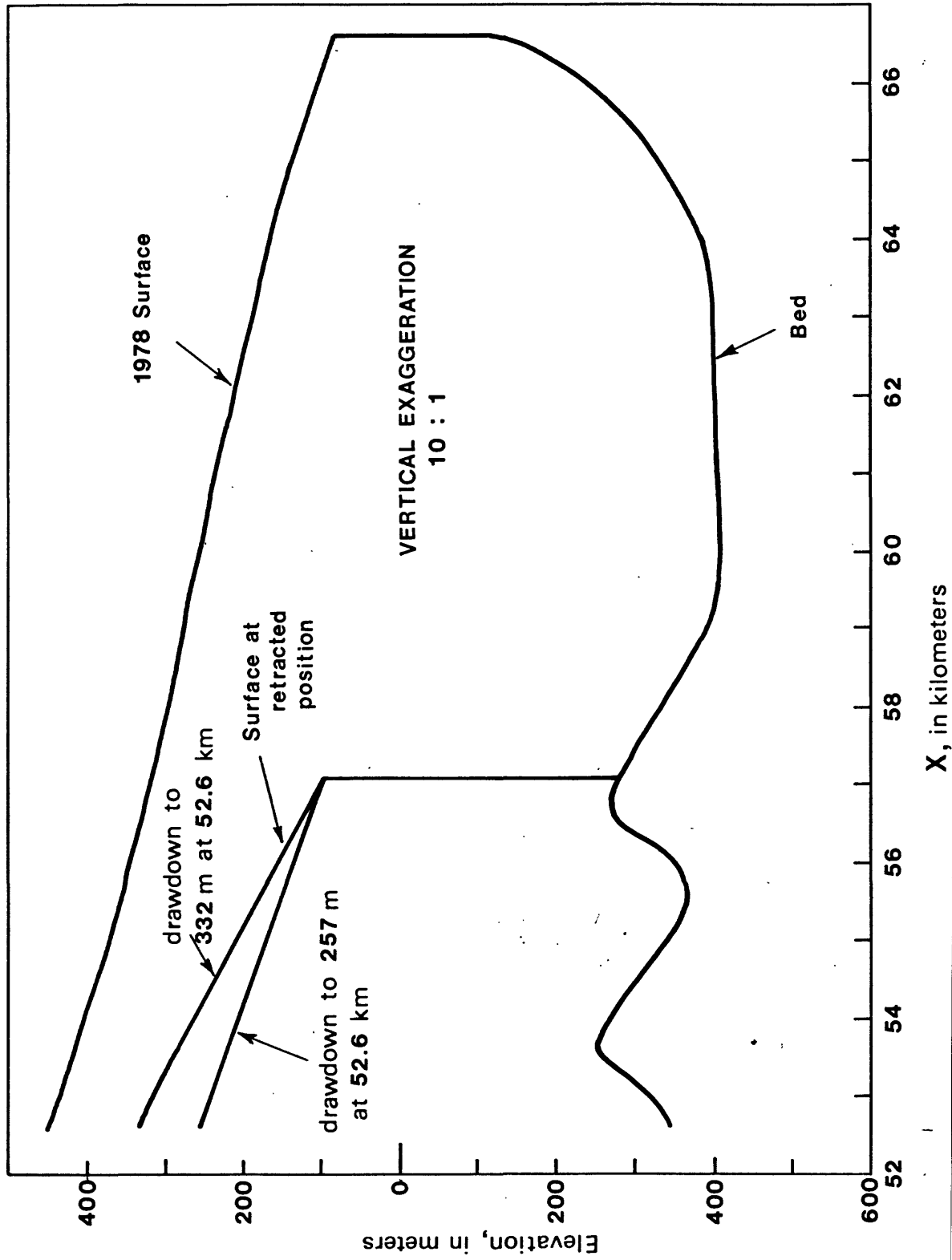


Figure 4.--Bed profiles and initial surface profile used in the models. Also shown are the two surface profiles assumed for the retracted position in the calving model calculations.

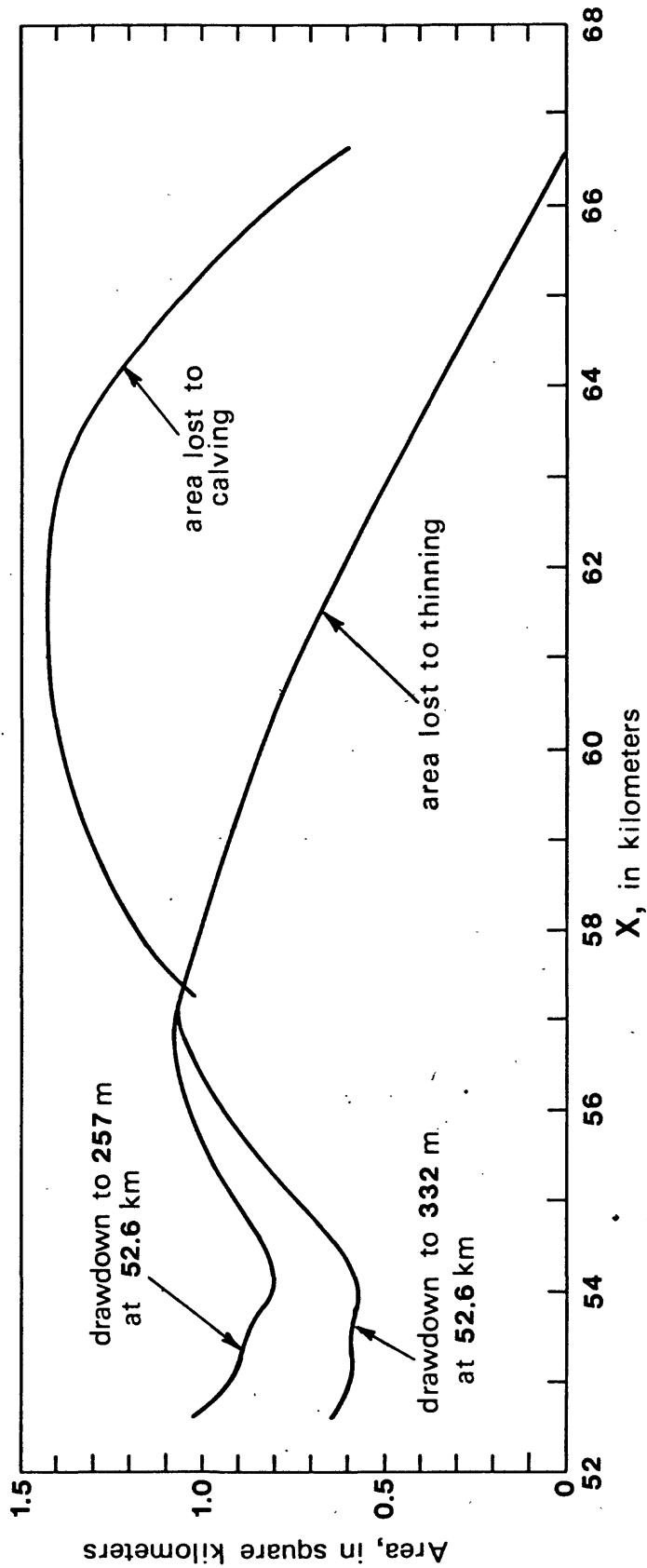


Figure 5.--Cross-sectional area lost due to calving (below  $z = h_g$  or to thinning (above  $z = h_g$ ) from the present profile to a retracted position.

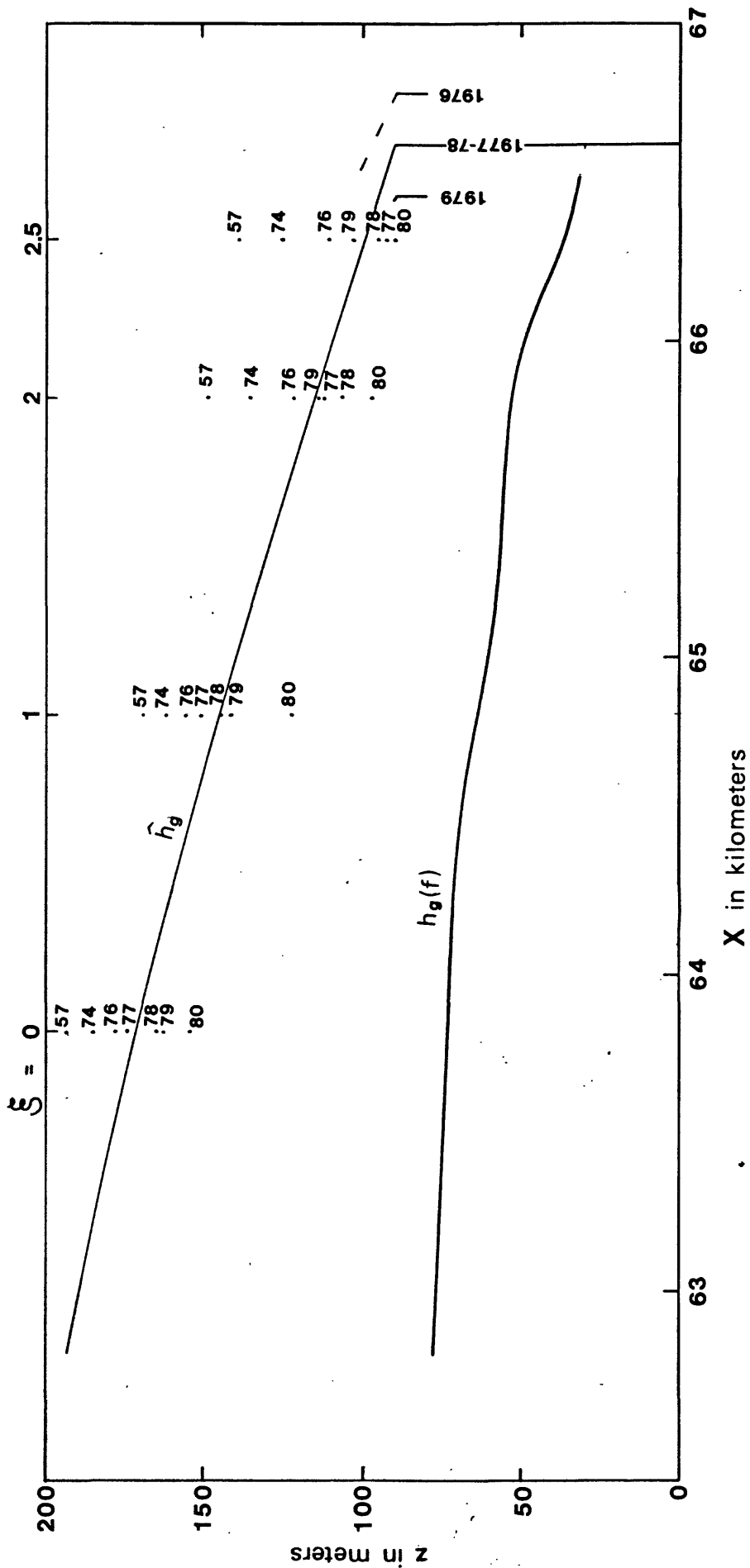


Figure 6.--Longitudinal profile of the lowest 4 kilometers of Columbia Glacier. The adjusted centerline surface profile is indicated by  $\hat{h}_g$ ; the height of the surface for the glacier to just float is indicated by  $h_g(f)$ . The numbers 57-80 indicate the actual surface profiles averaged over the width during late summer for the years 1957-79; the 80 value was measured February 29, 1980. Also shown is the position of the terminus in 1976, 1977, 1978, and 1979.

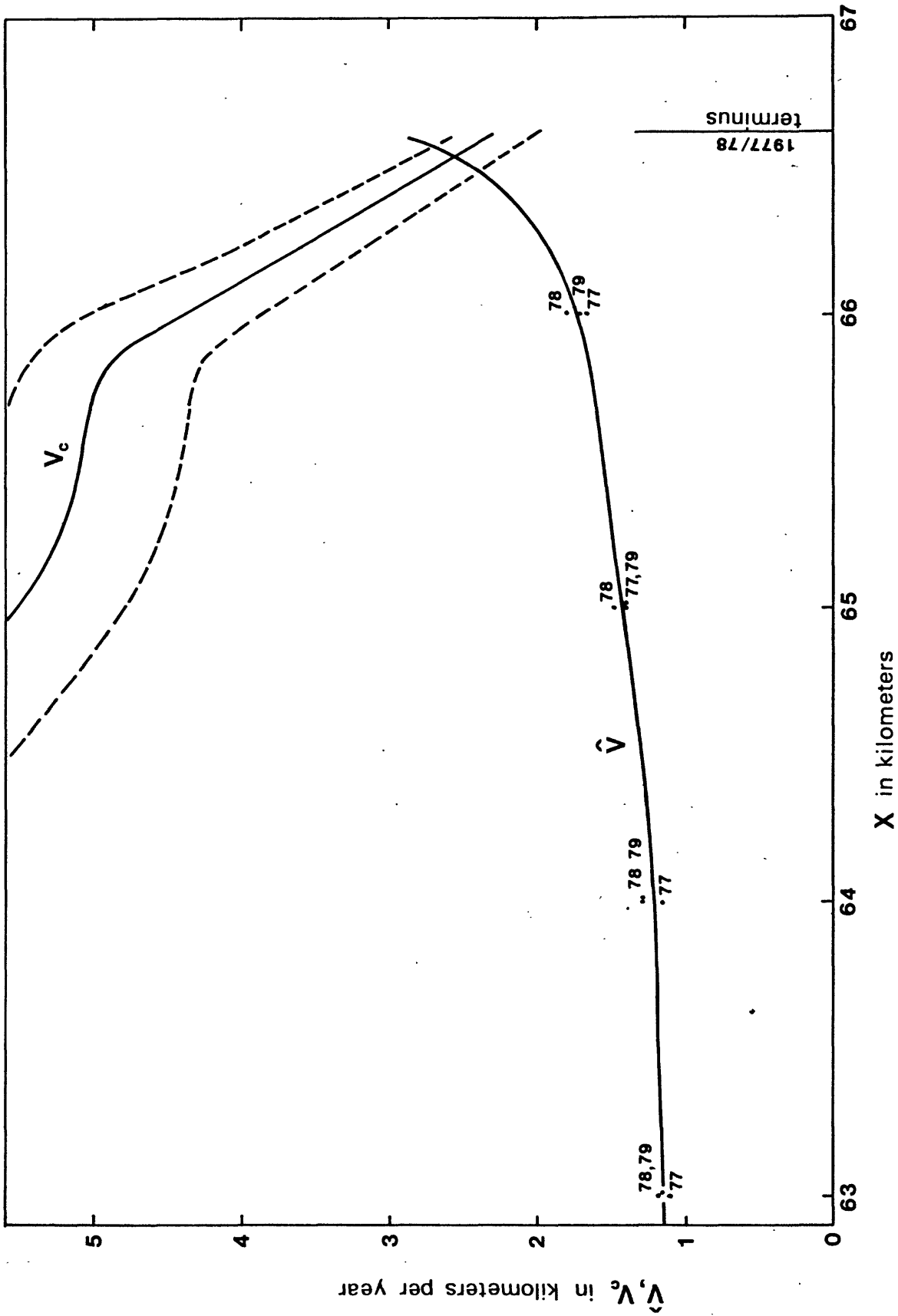


Figure 7.--Longitudinal profile of velocity  $\hat{V}$  from the adjusted data set, together with values averaged over a year centered on July 1 of 1977, 1978, and 1979. Also shown is the calving speed  $V_c$  together with 95 percent confidence limits.

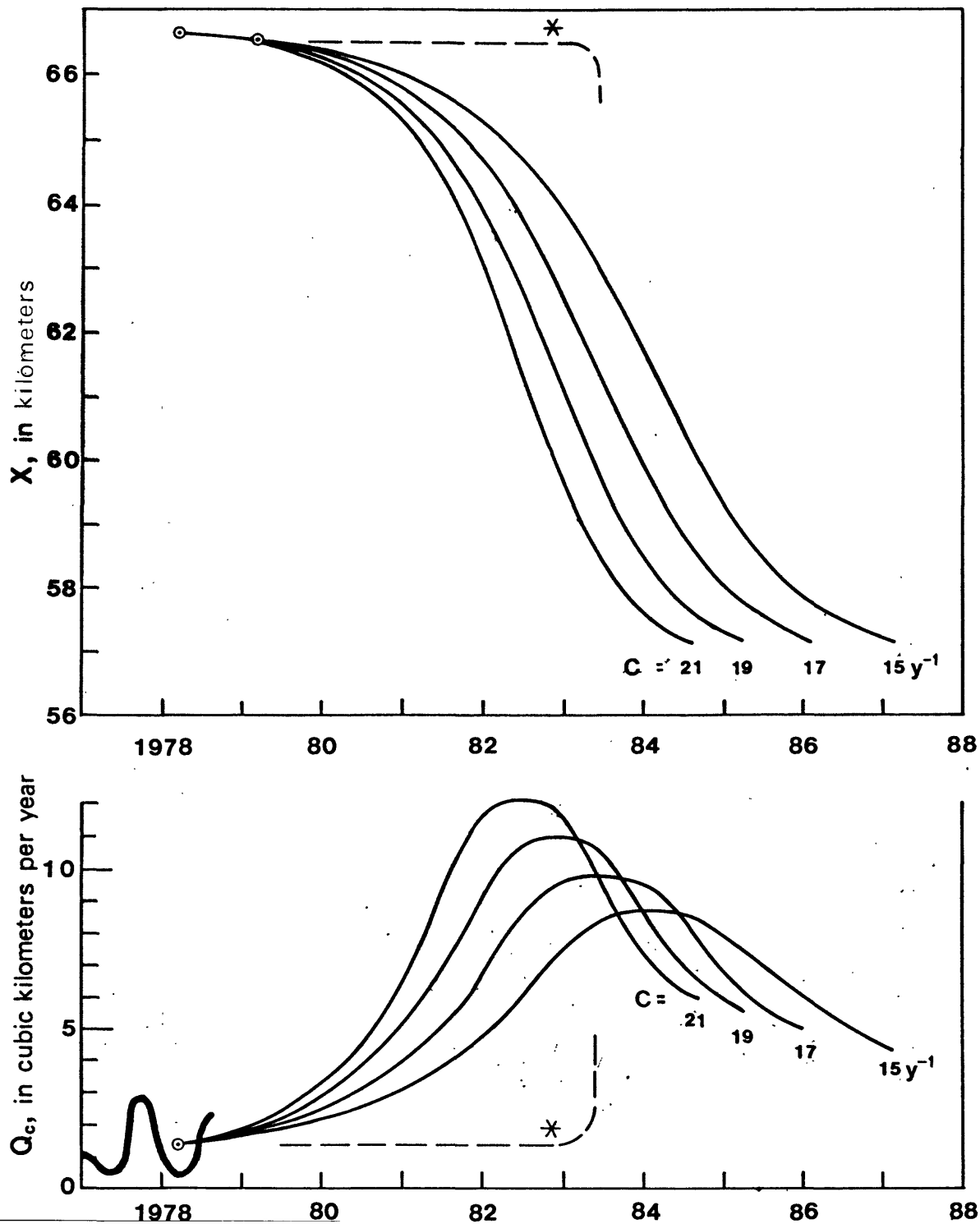


Figure 8.--Predicted time profiles of terminus position  $X$  and calving flux  $Q_c$  as functions of calving law coefficient  $c$ , for 1978-88, using  $10.0 \text{ km}^3$  drawdown. Known points are indicated by small circles, known fluctuation in  $Q_c$  indicated by heavy line. Dashed line shows predicted  $X$  and  $Q_c$  for dynamic model, assuming thinning to the point of floating (indicated by \*) for  $c = 16.9 \text{ y}^{-1}$ .

Table 1.--Current activity, width, and water depth at terminus; size; and accumulation-area ratio (AAR) for 33 large calving glaciers of Alaska. [Glacier locations are shown on figure 1.]

Glacier name and number	Terminus		Length			Total area km <sup>2</sup>	AAR	
	Activity <sup>1</sup>	Average water depth m	Width km	Extended position km	Retracted position km			Present Position km
1 McCarty	S	12	1.2	40	15	15	113	79
2 Northwestern	S	68	1	39	23	23	70	90
3 Holgate	S	20	0.6	21	14	14	67	92
4 Aialik	S	39	1.5	22	12	12	69	89
5 Chenega	S	150	2.1	33	27	27	371	94
6 Tiger	S	48	0.7	30	12	12	56	89
7 Nellie Juan	SR	20	1	18	14	15	56	91
8 Blackstone-Beloit	S	20	1	19	12	12	13	76
9 Harriman	A	3	1.7	45	11	13	76	65
10 Surprise	S	8	1	17	12	12	77	80
11 Serpentine	S	1	0.5	12	10	10	30	68

<sup>1</sup>A-Advancing  
S-Stable  
SR-Slow retreat  
RR-Rapid retreat

Table 1.--Current activity, width, and water depth at terminus; size; and accumulation-area ratio (AAR) for 33 large calving glaciers of Alaska--Continued--  
 [Glacier locations are shown on figure 1.]

Glacier name and number	Terminus		Length			Total area km <sup>2</sup>	AAR	
	Activity	Average water depth m	Width km	Extended position km	Retracted position km			Present position km
12 Barry	S	61	2	31	26	26	91	74
13 Harvard	A	36	2.5	76	28	40	578	80
14 Yale	RR	153	1.4	40	30	32	196	76
15 Meares	A	31	1.5	43	23	26	154	86
16 Columbia	S	75	8	66	35	66	1072	66
17 Shoup	SR	10	0.9	32	28	28	165	59
18 Guyot	RR	100	9	106	60	62	1544	91
19 Tyndall	RR	64	2	51	31	35	48	67
20 Hubbard	A	80	9	183	111	120	3914	96
21 Turner	A	20	4	93	34	35	54	73
22 Nunatak	S	0	1	97	36	36	72	59
23 Lituya	A	9	1	32	14	19	114	78

<sup>1</sup> A-Advancing  
 S-Stable  
 SR-Slow retreat  
 RR-Rapid retreat

Table 1.--Current activity, width, and water depth at terminus; size; and accumulation-area ratio (AAR) for 33 large calving glaciers of Alaska--Continued--  
 [Glacier locations are shown on figure 1.]

Glacier name and number	Terminus		Length				Total area km <sup>2</sup>	AAR
	Activity	Average water depth m	Width km	Extended position km	Retracted position km	Present position km		
24 North Crillon	A	8	0.4	34	14	19	121	78
25 La Perouse	S	0	3.6	25	25	25	153	65
26 Grand Pacific	A	18	2.4	170	113	116	660	72
27 Margerie	S	15	1.8	170	30	30	219	84
28 Johns Hopkins	A	56	1.6	149	111	113	322	91
29 Muir	RR	100	1	121	24	26	141	74
30 Taku	A	0	8	65	53	63	841	88
31 South Sawyer	RR	186	1	116	55	57	732	76
32 Dawes	RR	186	1.1	94	30	43	723	66
33 Le Conte	S	169	1.2	56	37	37	496	90

<sup>1</sup> A-Advancing  
 S-Stable  
 SR-Slow retreat  
 RR-Rapid retreat

Table 2.--Water depth  $h_w$ , ice surface height  $h_g$ , calving speed  $V_c$ , rate of advance  $\dot{X}$ , and buoyancy ratio  $\rho_w \hat{h}_w / \rho_i \hat{h}$  at the terminus of 12 glaciers.

[Value given above, standard error<sup>1</sup> given in parentheses. Values measured at centerline indicated by ( $\hat{\quad}$ ), otherwise values refer to average across width. Glacier locations are shown in figure 1, and are numbered as in table 1.]

Glacier number	Glacier name, date	$\hat{h}_w$ [m]	$\hat{h}_g$ [m]	$h_w$ [m]	$h_g$ [m]	$V_c$ [m/y]	$\dot{X}$ [m/y]	$\frac{\rho_w \hat{h}_w}{\rho_i \hat{h}}$	Analysis Method <sup>2</sup>
1	McCarty, 1964-65	14 (5)	32 (10)	12 (2)	30 (10)	600 (250)	0 (2)	.34	1
13	Harvard, 1977-78	57 (5)	72 (10)	36 (5)	68 (10)	1080 (400)	+10 (2)	.50	1
14	Yale, 1977-78	201 (20)	85 (10)	153 (25)	69 (10)	3500 (600)	-436 (10)	.80	1
15	Meares, 1977	63 (2)	74 (10)	31 (2)	59 (10)	1010 (270)	-34 (2)	.52	1
16	Columbia, 1977-78	134 (17)	90 (4)	75 (6)	86 (3)	2140 (100)	-1 (5)	.68	1
19	Tyndall, 1964-65	100 (8)	52 (10)	64 (10)	49 (10)	1740 (170)	-206 (10)	.74	1
20	Hubbard, 1977-78	100 (20)	120 (20)	80 (20)	92 (20)	2630 (200)	-32 (5)	.51	1

<sup>1</sup>Standard error determined or estimated from precision and density of measurements, possible lack of synchronicity between different measurements, and in case of ice speed, estimated seasonal or short-term speed fluctuations compared with time interval of measurement.

<sup>2</sup>1 using equation (1) directly, 2 using equations (3), (4), (1).

Table 2.--Water depth  $h_w$ , ice surface height  $h_g$ , calving speed  $V_c$ , rate of advance  $\dot{x}$ , and buoyancy ratio  $\rho_w \hat{h}_w / \rho_i \hat{h}$  at the terminus of 12 glaciers--Continued

[Value given above, standard error<sup>1</sup> given in parentheses. Values measured at centerline indicated by ( $\hat{\quad}$ ), otherwise values refer to average across width. Glacier locations are shown in figure 1, and are numbered as in table 1.]

Glacier number	Glacier name, date	$\hat{h}_w$ [m]	$\hat{h}_g$ [m]	$h_w$ [m]	$h_g$ [m]	$V_c$ [m/y]	$\dot{x}$ [m/y]	$\frac{\rho_w \hat{h}_w}{\rho_i \hat{h}}$	Analysis Method <sup>2</sup>
26	Grand Pacific, 1968-70	34 (8)	47 (8)	18 (10)	44 (7)	220 (70)	+28 (2)	.48	1
27	Margerie, 1977	34 (8)	64 (10)	15 (8)	60 (10)	463 (100)	0 (2)	.39	1
28	Johns Hopkins, 1979	84 (2)	74 (10)	56 (2)	70 (13)	2290 (800)	-50 (2)	.60	1
29	Muir, 1979	137 (10)	64 (7)	100 (10)	60 (10)	3700 (2000)	-600 (12)	.77	1
31	South Sawyer, 1960-71	220 (30)	51 (10)	186 (30)	48 (10)	3200 (1000)	-1500 (1000)	.92	1
1a	McCarty, 1942-50	268 (5)	60 (25)	172 (5)	48 (5)	4200 (1100)	-1225 (25)	.92	2
1b	McCarty, 1950-60	87 (2)	35 (10)	60 (2)	32 (10)	2980 (800)	-160 (3)	.81	2

<sup>1</sup>Standard error determined or estimated from precision and density of measurements, possible lack of synchronicity between different measurements, and in case of ice speed, estimated seasonal or short-term speed fluctuations compared with time interval of measurement.

<sup>2</sup>1 using equation (1) directly, 2 using equations (4), (5), (1).

Table 2.--Water depth  $h_w$ , ice surface height  $h_g$ , calving speed  $V_c$ , rate of advance  $\dot{x}$ , and buoyancy ratio  $\rho_w \hat{h}_w / \rho_i \hat{h}$  at the terminus of 12 glaciers--Continued

[Value given above, standard error<sup>1</sup> given in parentheses. Values measured at centerline indicated by (^), otherwise values refer to average across width. Glacier locations are shown in figure 1, and are numbered as in table 1.]

Glacier number	Glacier name, date	$\hat{h}_w$ [m]	$\hat{h}_g$ [m]	$h_w$ [m]	$h_g$ [m]	$V_c$ [m/y]	$\dot{x}$ [m/y]	$\frac{\rho_w \hat{h}_w}{\rho_i \hat{h}}$	Analysis Method <sup>2</sup>
26a	West Glacier Bay, 1860-79	408 (30)	90 (40)	292 (30)	68 (40)	10700 (3500)	-1680 (250)	.93	2 <sup>3</sup>
29a	Muir, 1892-1948	267 (5)	85 (30)	180 (5)	68 (4)	3490 (950)	-450 (9)	.86	2
29b	Muir, 1948-72	244 (2)	80 (30)	173 (2)	64 (3)	4020 (1100)	-379 (8)	.85	2

<sup>1</sup>Standard error determined or estimated from precision and density of measurements, possible lack of synchronicity between different measurements, and in case of ice speed, estimated seasonal or short-term speed fluctuations compared with time interval of measurement.

<sup>2</sup>1 using equation (1) directly, 2 using equations (4), (5), (1).

<sup>3</sup>Thickness-change flux derived from topographic maps constructed from estimated longitudinal profiles based on known bed topography, known terminus position, and the assumption of constant basal shear stress.

Table 3.--Calving law forms and coefficients fitted to the data given in table 2.--Continued. Also given is the standard error of estimate of the coefficient  $\sigma_c$  and the variance reduction fraction

$F = 1 - [\sum_i (V_{ci} - V_c)^2 / \sum_i (V_{ci} - \bar{V}_c)^2]$ , where  $V_c$  is the value predicted by the relationship,  $\bar{V}_c$  is the mean observed value, and the sum is over the observed  $V_{ci}$ . For those two-parameter formulae equivalent to linear regressions (such as  $V_c = \hat{c}h_w + a$  or  $V_c = \hat{c}h_w^\alpha$ ),  $F=r^2$ , the coefficient of determination. Units of  $c$  assume  $V_c$  in m/y, and  $h, h_w$  in m. For some cases, the coefficient  $c$  and statistical measures  $\sigma_c$  and  $F$  are calculated with weighted data from table 2, in which the weight =  $[c^2 e_h^2 + e_v^2]^{-1}$  where  $e_h$  is the standard error in  $h$  or  $h_w$  and  $e_v$  is the standard error in  $V_c$ .

		Method 1 <sup>1</sup> [12 cases]		Methods 1 and 2 <sup>1</sup> [17 cases]	
		Unweighted	Weighted	Unweighted	Weighted
$V_c = \hat{c}h_w$	$c$	18.41	17.03	19.76	16.94
	$F$	.77	.85	.81	.84
	$\sigma_c$	1.46	1.10	1.47	.99
$V_c = ch_w$	$c$	24.38	27.97	27.86	27.11
	$F$	.69	.91	.81	.89
	$\sigma_c$	2.25	1.71	2.01	1.95
$V_c = \hat{c}h$	$c$	11.77	8.38	14.33	9.08
	$F$	.77	.68	.74	.68
	$\sigma_c$	.98	.65	1.22	.70
$V_c = c \frac{\rho_w}{\rho_i} \frac{\hat{h}_w}{\hat{h}}$	$c$	3303.		4470.	
	$F$	.56		.38	
	$\sigma_c$	373.		642.	
$V_c = c(2\hat{h} - \hat{h}_w)$	$c$	8.18		10.97	
	$F$	.61		.65	
	$\sigma_c$	.69		1.42	
$V_c = \frac{\hat{c}h_w}{\rho_i \hat{h} - \rho_w \hat{h}_w}$	$c$	472.		580.	
	$F$	-.36		.52	
	$\sigma_c$	114.		67.	
$V_c = \frac{c}{\rho_i \hat{h} - \rho_w \hat{h}_w}$	$c$	67855.		97008.	
	$F$	-.42		-.05	
	$\sigma_c$	16527.		22695.	

<sup>1</sup>Method 1 uses equation (1) directly; Method 2 uses equations (3), (4), and (1).

Table 3.--Calving law forms and coefficients fitted to the data given in table 2. Also given is the standard error of estimate of the coefficient  $\sigma_c$  and the variance reduction fraction

$F = 1 - [\sum_i (V_{ci} - V_c)^2 / \sum_i (V_{ci} - \bar{V}_c)^2]$ , where  $V_c$  is the value predicted by the relationship,  $\bar{V}_c$  is the mean observed value, and the sum is over the observed  $V_{ci}$ . For those two-parameter formulae equivalent to linear regressions (such as  $V_c = ch_w + a$  or  $V_c = ch_w^\alpha$ ),  $F=r^2$ , the coefficient of determination. Units of  $c$  assume  $V_c$  in m/y, and  $h, h_w$  in m. For some cases, the coefficient  $c$  and statistical measures  $\sigma_c$  and  $F$  are calculated with weighted data from table 2, in which the weight =  $[c^2 e_h^2 + e_v^2]^{-1}$  where  $e_h$  is the standard error in  $h$  or  $h_w$  and  $e_v$  is the standard error in  $V_c$ .

		Method 1 <sup>1</sup> [12 cases]		Methods 1 and 2 <sup>1</sup> [17 cases]	
		Unweighted	Weighted	Unweighted	Weighted
$V_c = \frac{c \hat{h}}{\rho_i \hat{h} - \rho_w \hat{h}_w}$	$c$	620.		520.	
	$F$	.01		.60	
	$\sigma_c$	121.		61.	
$V_c = \frac{c \hat{h}_g}{\rho_i \hat{h} - \rho_w \hat{h}_w}$	$c$	1354.		1897.	
	$F$	.19		.44	
	$\sigma_c$	220.		252.	
$V = ch_w^a$	$c$	23.02		23.27	
	$a$	.95		.95	
	$F$	.73		.79	
$V = ch^a$	$c$	1.14		1.66	
	$a$	1.42		1.36	
	$F$	.72		.75	
$V = ch_w + a$	$c$	16.53		20.14	
	$a$	258.		-84.	
	$F$	.78		.81	

<sup>1</sup>Method 1 uses equation (1) directly; Method 2 uses equations (3), (4), and (1).